EFFICIENCY AND RELIABILITY ENHANCEMENTS IN PROPULSION FLOWFIELD MODELING

Philip E.O. Buelow,* Sankaran Venkateswaran,† Charles L. Merkle‡
Propulsion Engineering Research Center
Department of Mechanical Engineering
The Pennsylvania State University

SUMMARY:

The implementation of traditional CFD algorithms in practical propulsion related flowfields often leads to dramatic reductions in efficiency and/or robustness. The present research is directed at understanding the reasons for this deterioration and finding methods to circumvent it. Work to date has focussed on low Mach number regions, viscous dominated regions and high grid aspect ratios. Time derivative preconditioning, improved definition of the local time stepping, and appropriate application of boundary conditions are employed to decrease the required time to obtain a solution, while maintaining accuracy. A number of cases having features typical of rocket engine flowfields are computed to demonstrate the improvement over conventional methods. These cases include laminar and turbulent high Reynolds number flat plate boundary layers, flow over a backward-facing step, a diffusion flame, and wall heat-flux calculations in a turbulent converging-diverging nozzle. Results from these cases show convergence that is virtually independent of the local Mach number and the grid aspect ratio, which translates to a convergence speed-up of up to several orders of magnitude over conventional algorithms. Current emphasis is in extending these results to three-dimensional flows with highly stretched grids.

TECHNICAL DISCUSSION:

Propulsion flowfields contain a rich variety of physical processes. The combustion process in a rocket engine takes place at low flow speeds and is accompanied by very high rates of energy release and species generation. Although the Reynolds numbers are high, mixing and diffusion are critical to achieving combustion, and recirculation regions are often present near the injector face. Following combustion, the flow accelerates through the nozzle to supersonic speeds, where the Reynolds numbers are typically very high and there is little heat release, but recombination effects are important for performance predictions. This wide variety of physical processes and conditions presents a formidable challenge for CFD codes.

In order to design an efficient and reliable CFD code to solve these flowfields, one needs to address the issues which lead to a deterioration in code performance. Convergence rates and code robustness often suffer in practical problems due to any number of factors. For example, the initial conditions may be poorly specified, the grid resolution may be inadequate, very high grid stretching will generally be present, or there may be flow regimes present for which the algorithm was not designed to converge efficiently. An example of this latter issue occurs for traditional density-based algorithms in the presence of very low Mach numbers, as occurs in the combustion chamber. Density-based algorithms were designed for transonic and supersonic Mach number flows, but typically have difficulty computing low Mach number flows. The convergence rates of these algorithms decrease dramatically because of the wide disparity

---

*Graduate Research Assistant
†Research Associate
‡Distinguished Alumni Professor

130

between fluid particle and acoustic wave propagation speeds. Various researchers, including the present authors, have negated these detrimental effects through the use of time-derivative preconditioning [1-6] so that such schemes are now routinely used at low speeds. A related issue at low Reynolds numbers occurs where the disparity between wave propagation speeds and viscous diffusion rates controls the convergence. This has also been effectively addressed through time-derivative preconditioning [2,3,6].

The details of the preconditioning techniques used herein can be found in References [2],[3] and [7]. The basic technique is to premultiply the time derivative by an appropriate preconditioning matrix. For flows dominated by inviscid effects, the preconditioning matrix is designed to alter the acoustic speed of the governing system so that each of the inviscid time scales is of the same order. This allows a larger time step than the unaltered system. The preconditioned density-based system closely resembles a 'pressure-based' system at low Mach numbers, while reverting to the traditional density-based system at transonic and supersonic Mach numbers [8]. For viscous flows, there exists a time-scale disparity between the diffusive and the convective processes. At low Reynolds numbers, this disparity becomes strong enough to deteriorate the convergence rate. Typically the difficulty arises when the cell Reynolds number (e.g. $Re_{\Delta x} = u\Delta x/\nu$) becomes less than unity. Such Reynolds numbers are encountered in boundary layers, shear layers, recirculation regions, or anywhere the flow gradients are strong. In this case the previous preconditioning matrix is slightly altered so that the acoustic time scale is of the same order as the diffusive time scale [2].

It is also well known that the presence of large grid aspect ratios decreases the performance of conventional algorithms. Large grid aspect ratios are often required to resolve the steep gradients that occur in turbulent boundary layer calculations. Flow calculations in long, narrow ducts also give rise to large grid aspect ratios. The decreased performance in the presence of large grid aspect ratios occurs because of a wide disparity in the cell crossing times in the different coordinate directions. The difficulties caused by the large grid aspect ratios have been addressed by the present authors [7], and resulted in improvements that yield convergence rates that are orders of magnitude faster than the conventional algorithms in highly stretched grids for two-dimensional problems. Presently, these improvements only apply to the 2-D ADI scheme. In order to obtain enhanced convergence, three issues must be addressed. The choice of the local time step should be based on the minimum CFL number

$$\Delta t = \text{Max} \left[\frac{\text{CFL}\Delta x}{\lambda_x}, \frac{\text{CFL}\Delta y}{\lambda_y} \right]$$

where λ_x and λ_y are the acoustic eigenvalues in each of the coordinate directions. The boundary conditions should be applied before the governing equations are approximately factored, and the viscous preconditioning should be based upon the maximum von Neumann number, VNN (see Ref. [7]).

RESULTS:

To demonstrate the efficiency and reliability of the improved algorithm, the following test cases are presented: 1) turbulent flat plate boundary layer, 2) H_2/O_2 diffusion flame, 3) 2-D backward facing step, 4) turbulent rocket nozzle heat flux computation. Additional cases have been calculated; however, they are not presented here because of space limitations.

The first case is a Mach 0.1 turbulent flat plate boundary layer computation. The Reynolds number for this case is 8×10^5, and the maximum grid aspect ratio (located adjacent to the wall) is 8000. The k-ϵ turbulence model was used for closure. Figure 1 displays the convergence history for the enhanced ADI algorithm (preconditioning + grid aspect ratio enhancements), and for the standard ADI algorithm. The enhanced algorithm converges in under 2000 steps, whereas the convergence for the standard algorithm flattens after a three order of magnitude drop in the residual and would require over 50,000 steps to converge to machine accuracy.

The H_2/O_2 diffusion flame consists of a central core flow of pure oxygen (Reynolds number of 200). The outer gas flow is pure hydrogen. The grid size used is 71 × 61. Both reacting and nonreacting cases were computed, and the convergence for both cases using the enhanced algorithm are shown in Figure 2. For the reacting case, the reaction rates were reduced for initial start-up and gradually increased to their full level, which is represented by the initial portion of the convergence curve. Once the reactions are at the full level, the convergence rate is the same as the nonreacting case. Figure 3 shows contours of temperature and water mass fractions for the reacting case.

The geometry for the 2-D backward facing step corresponds to the one studied experimentally by Armaly et al. [9]. The length and width of the duct are 10 cm and 1 cm respectively, and the step height is 0.5 cm. A uniform grid of 101 × 61 is used. Convergence results are shown in Figure 4 for Re = 100, 200, 300 and 400. The residuals are shown sequentially because each case is used as the initial condition for the subsequent case. All Reynolds number cases converge at about the same rate of 7 orders of magnitude in 1000 steps. Table 1 shows the predicted primary recirculation zone lengths, normalized by the step height. Agreement between computations and measurements is excellent.

The final case shown is high Reynolds number turbulent flow through a converging-diverging nozzle with cooled walls. The incoming gas is at a stagnation temperature of 3500 K and the wall is maintained at 700 K. The grid size is 141 × 121. For accuracy in heat flux predictions it is necessary to maintain a minimum y^+ of about one along the wall. The strong wall stretching results in grid aspect ratios that are as high as 2×10^6 in this region. Figure 5 shows the convergence for the standard algorithm and the enhanced algorithm. The enhanced algorithm converges in 2000 steps, whereas the standard algorithm would require over 50,000 steps to reach machine accuracy. Even though the standard algorithm converges about five orders of magnitude in 4000 steps, Figure 6 reveals that the wall heat flux is far from converged. In fact, even after 20,000 steps the wall heat flux is not quite fully converged in the throat region. This is because the convergence in the near wall region is much slower than the core flow due to the extremely large aspect ratios near the wall. Examination of the wall heat fluxes from the enhanced algorithm reveals that a fully converged solution is reached in just 400 iterations, indicating the flowfield in the near wall region and the core region converge at similar rates.

REFERENCES:

1. Turkel, E., "Review of Preconditioning Methods for Fluid Dynamics," NASA Contractor Report 189712, ICASE Report No. 92-47.

2. Choi, Y-H. and Merkle, C. L., "The Application of Preconditioning to Viscous Flows," *Journal of Computational Physics*, Vol. 105, No. 2, April, 1993, pp. 207-223.

3. Venkateswaran, S., Weiss, J.M., Merkle, C. L. and Choi, Y.-H., "Propulsion-Related Flowfields Using the Preconditioned Navier-Stokes Equations," AIAA Paper 92-3437, July, 1992.

4. Shuen, J.-S., Chen, K.-H. and Choi, Y.-H., "A Time-Accurate Algorithm for Chemical Non-Equilibrium Viscous Flows at All Speeds," AIAA 92-3639, July, 1992.

5. van Leer, B., Lee, W. T. and Roe, P. L., "Characteristic Time-Stepping or Local Preconditioning of the Euler Equations," AIAA Paper 91-1552, June, 1991.

6. Godfrey, A. G., Walters, R. W. and van Leer, B., "Preconditioning for the Navier-Stokes Equations," AIAA Paper 93-0535, January, 1993.

7. Buelow, P.E.O., Venkateswaran, S. and Merkle, C. L., "The Effect of Grid Aspect Ratio on Convergence," AIAA Paper 93-3367, July, 1993.

8. Merkle, C. L., Venkateswaran, S. and Buelow, P. E. O., "The Relationship Between Pressure-Based and Density-Based Algorithms," AIAA 92-0425, 30th Aerospace Sciences Meeting, January, 1992, Reno, NV.
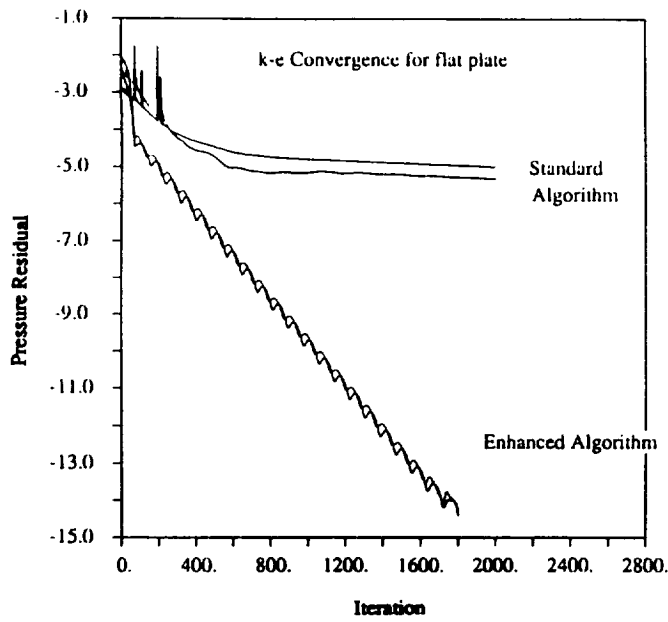
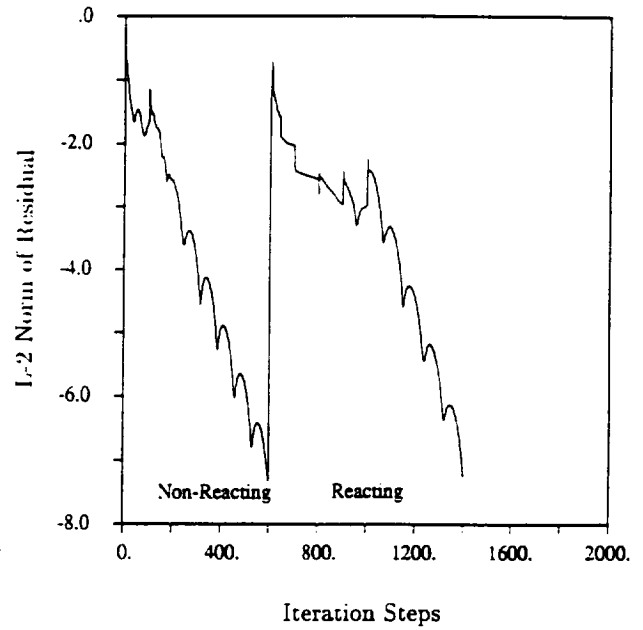Figure 1: Convergence for turbulent flat plate boundary layer for standard and enhanced algorithm

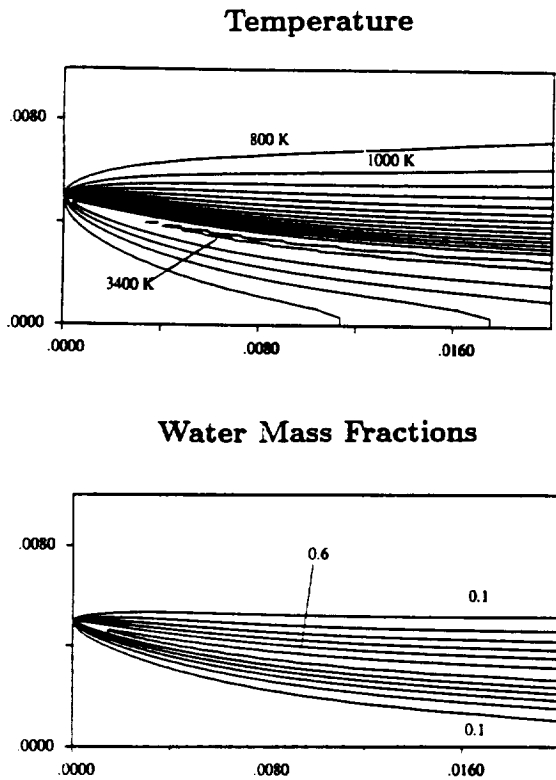Figure 2: Convergence for nonreacting and reacting multi-species shear layer

Figure 3: Contours of temperature and H_2O mass fractions for the reacting shear layer
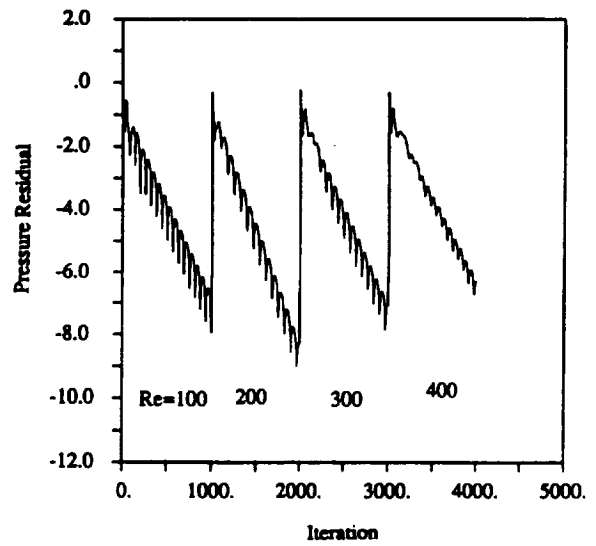

Figure 4: Convergence for backward facing step at various Reynolds numbers

133

Table I.
Reattachment Length vs. Reynolds Number for Backward Facing Step

Reattachment Length, X_r/S

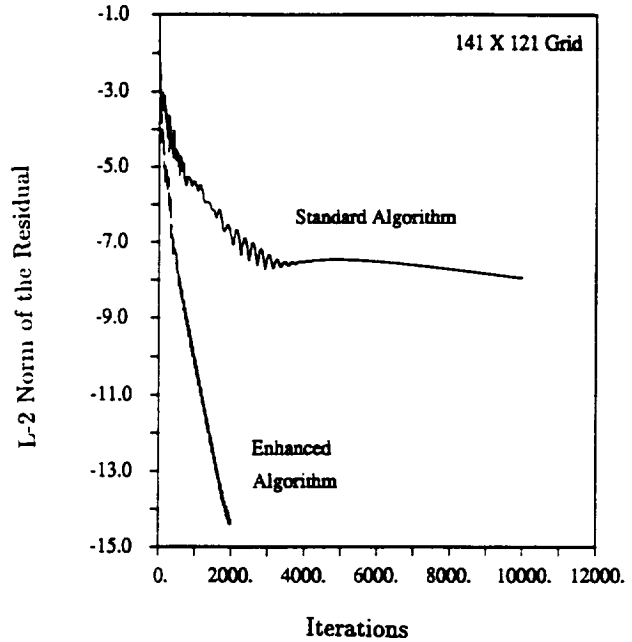| Reynolds No.	Experiment [22]	Implicit
100	3.0	3.0
200	5.0	5.0
300	6.8	6.6
400	8.6	8.0

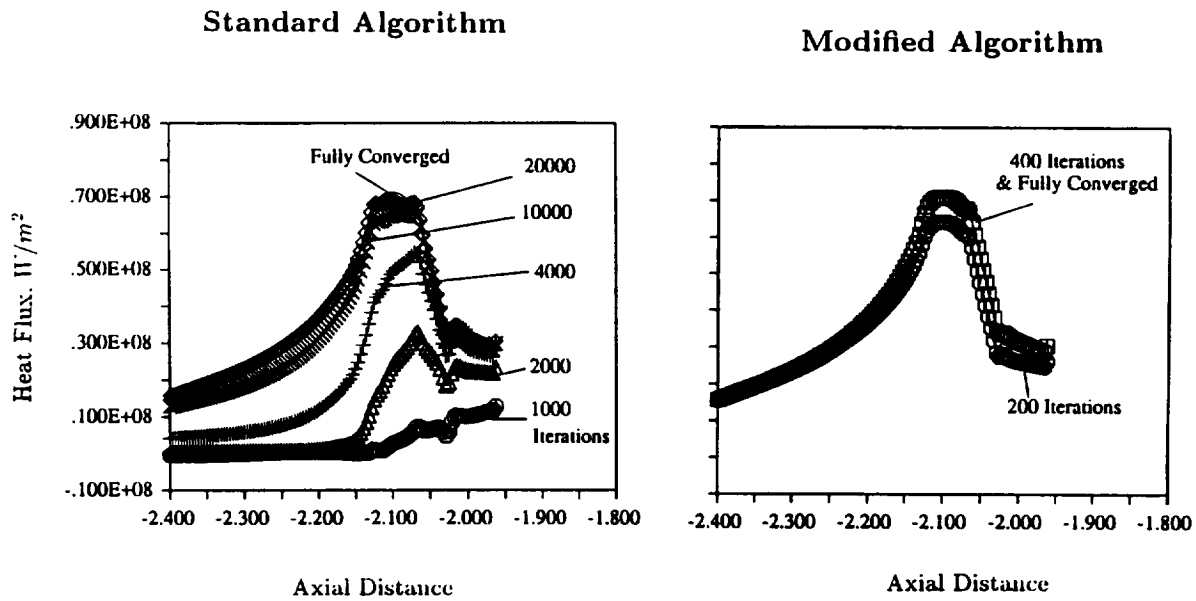Figure 5: Convergence for turbulent nozzle computations for standard and enhanced algorithms

Figure 6: Wall heat flux results for standard and enhanced algorithms